Radiotherapy and Oncology 157 (2021) 15–23

Contents lists available at ScienceDirect

Radiotherapy and Oncology

journal homepage: www.thegreenjournal.com

Original Article

Modelling of late side-effects following cranial proton beam therapy

Almut Dutz [a,b], Armin Lühr [a,b,c], Linda Agolli [a,d], Rebecca Bütof [a,d,e], Chiara Valentini [a,d], Esther G.C. Troost [a,b,c,d,e], Michael Baumann [a,b,c,d,e,f], Xavier Vermeren [g], Dirk Geismar [g,h,i], Nayan Lamba [j], Emily S. Lebow [j], Meghan Bussière [j], Jillian E. Daly [j], Marc R. Bussière [j], Mechthild Krause [a,b,c,d,e,1], Beate Timmermann [g,h,i,k,1], Helen A. Shih [j,1], Steffen Löck [a,c,d,1,*]

[a] OncoRay – National Center for Radiation Research in Oncology, Faculty of Medicine and University Hospital Carl Gustav Carus, Technische Universität Dresden, Helmholtz-Zentrum Dresden - Rossendorf, Dresden, Germany; [b] Helmholtz-Zentrum Dresden - Rossendorf, Institute of Radiooncology – OncoRay, Dresden; [c] German Cancer Consortium (DKTK), partner site Dresden, and German Cancer Research Center (DKFZ), Heidelberg; [d] Department of Radiotherapy and Radiation Oncology, Faculty of Medicine and University Hospital Carl Gustav Carus, Technische Universität Dresden; [e] National Center for Tumor Diseases (NCT), partner site Dresden, Germany German Cancer Research Center (DKFZ), Heidelberg, Germany; Faculty of Medicine and University Hospital Carl Gustav Carus, Technische Universität Dresden, Dresden, Germany, and; Helmholtz Association/Helmholtz-Zentrum Dresden - Rossendorf (HZDR), Dresden; [f] Deutsches Krebsforschungszentrum (DKFZ), Heidelberg, Germany; [g] West German Proton Therapy Center Essen (WPE); [h] Department of Particle Therapy; [i] West German Cancer Center (WTZ), University Hospital Essen, Germany; [j] Department of Radiation Oncology, Massachusetts General Hospital and Harvard Medical School, Boston, USA; [k] German Cancer Consortium (DKTK), partner site Essen, Germany

ARTICLE INFO

Article history:
Received 9 July 2020
Received in revised form 4 January 2021
Accepted 5 January 2021
Available online 19 January 2021

Keywords:
NTCP models
Brain tumours
Late side-effects
Proton beam therapy

ABSTRACT

Background: The limited availability of proton beam therapy (PBT) requires individual treatment selection strategies that can be based on normal tissue complication probability (NTCP) models. We developed and externally validated NTCP models for common late side-effects following PBT in brain tumour patients to optimise patients' quality of life.

Methods: Cohorts from three PBT centres (216 patients) were investigated for several physician-rated endpoints at 12 and 24 months after PBT: alopecia, dry eye syndrome, fatigue, headache, hearing and memory impairment, and optic neuropathy. Dose-volume parameters of associated normal tissues and clinical factors were used for logistic regression modelling in a development cohort. Statistically significant parameters showing high area under the receiver operating characteristic curve (AUC) values in internal cross-validation were externally validated. In addition, analyses of the pooled cohorts and of time-dependent generalised estimating equations including all patient data were performed.

Results: In the validation study, mild alopecia was related to high dose parameters to the skin [e.g. the dose to 2% of the volume (*D2%*)] at 12 and 24 months after PBT. Mild hearing impairment at 24 months after PBT was associated with the mean dose to the ipsilateral cochlea. Additionally, the pooled analyses revealed dose–response relations between memory impairment and intermediate to high doses to the remaining brain as well as *D2%* of the hippocampi. Mild fatigue at 24 months after PBT was associated with *D2%* to the brainstem as well as with concurrent chemotherapy. Moreover, in generalised estimating equations analysis, dry eye syndrome was associated with the mean dose to the ipsilateral lacrimal gland.

Conclusion: We developed and in part validated NTCP models for several common late side-effects following PBT in brain tumour patients. Validation studies are required for further confirmation.

 Radiotherapy and Oncology 157 (2021) 15–23

Proton beam therapy (PBT) can achieve high dose conformity with a simultaneous dose reduction in healthy tissues surrounding the tumour compared to conventional photon radiotherapy (XRT). These features may result in reduced side-effects and improved quality of life [1–5]. Although the number of PBT centres continues to increase [6], the broad availability of PBT is limited by the high costs associated with them. A selection of patients benefiting most likely from PBT is therefore required. One possible strategy for treatment selection is the "model-based approach", which is based on the prediction and comparison of normal tissue complication probabilities (NTCP) for XRT and PBT treatment plans [7–9]. The model-based approach has been implemented in the Netherlands and Denmark for certain tumour entities. However, it is not yet applied for cranial irradiation.

Modelled late side-effects of cranial XRT include radiation necrosis [10,11], cognitive deterioration [12,13], cranial neuropathies [14], endocrine dysfunction [15,16], hearing impairment

* Corresponding author at: OncoRay – National Center for Radiation Research in Oncology, Fetscherstr. 74, PF 41, 01307 Dresden, Germany.
E-mail address: Steffen.Loeck@oncoray.de (S. Löck).
[1] Shared last authorship.

https://doi.org/10.1016/j.radonc.2021.01.004
0167-8140/

[10,16,17], visual impairment [10,18,19], and other ocular injury [20]. However, due to fundamental differences in dose distributions and relative biological effectiveness (RBE), NTCP models derived from XRT data may not apply to PBT. While some XRT-based NTCP models performed well in PBT cohorts [21], others did not [22]. So far, published data regarding models in the setting of PBT are very limited [16,23].

Thus, we investigated common late side-effects up to two years after PBT that may affect patients' quality of life [24–29]: alopecia, dry eye syndrome, fatigue, headache, hearing and memory impairment, and optic neuropathy. PBT-based NTCP models in an exploration/validation setting and on pooled cohorts were developed. Additionally, time-dependent analyses including all follow-up data were performed.

Patients and methods

Patient data

Patient data from three institutes were analysed retrospectively. Cohort 1 consisted of 80 patients treated within clinical studies (DRKS00007670 [30] and DRKS00008569 [31]) between 12/2014 and 12/2017 at the Department of Radiotherapy and Radiation Oncology of the University Hospital Carl Gustav Carus Dresden. Cohort 2 comprised 53 patients from the West German Proton Therapy Centre Essen (treated 08/2013–08/2016 within the clinical registry study DRKS00004384 [32]) and cohort 3 consisted of 83 patients treated at Massachusetts General Hospital in Boston, MA, USA (treated 11/2013–12/2015). All patients were over 18 years of age, had a histologically confirmed primary brain tumour or tumour of the skull base, and were treated with normo-fractionated PBT with or without chemotherapy (temozolomide). The study was approved by the local Ethics Committee (EK566122019) and the institutional review board at the external institutions. Cohorts 1 and 2 were combined to a single exploration cohort to increase the number of patients for model development, while cohort 3 was used as a validation cohort. Exploration and validation cohorts are characterised in Table 1.

Treatment planning and delivery

Treatment plans were calculated using a double scattering PBT technique for cohort 1 and cohort 3 (except for two cases) and an active scanning technique for cohort 2 (two cases of cohort 3). For delineation and treatment planning, a computed tomography (CT) scan was acquired for each patient and rigidly registered with (post-operative) magnetic resonance imaging (MRI) scans. Gross tumour volumes encompassed the macroscopic tumour or the resection cavity including the residual tumour, if present. Clinical target volumes (CTVs) included microscopic disease and oedema (for malignant tumours) and were created considering tumour histology as well as anatomical boundaries. The dose-volume constraints differed slightly between cohorts 1 and 2 (supplementary Table S1); in cohort 3, patient-specific planning objectives were used. Further details on treatment planning and delivery were reported previously [33]. A constant RBE of 1.1 was assumed.

Table 1
Patient characteristics of the exploration cohort and the validation cohort for the analysis of late side-effects at 12 months and at 24 months after PBT.

	12 months following PBT					**24 months following PBT**				
	Exploration cohort		**Validation cohort**			**Exploration cohort**		**Validation cohort**		
Total number of patients	**104**		**67**			**74**		**65**		
Characteristics	**Median**	**(Range)**	**Median**	**(Range)**	***p*-value**	**Median**	**(Range)**	**Median**	**(Range)**	***p*-value**
Age[1] at PBT in years	48.2	(18.1–84.7)	45.9	(21.6–89.3)	0.22	45.3	(18.1–78.0)	47.0	(21.9–78.2)	0.93
Target volume (CTV)[1] in cm^3	71.3	(1.2–498.0)	29.6	(1.2–267.2)	0.003	61.2	(1.2–370.7)	29.4	(2.7–267.2)	0.015
Total dose[1] in Gy(RBE)	54.0	(30.0–74.0)	54.0	(45.0–70.2)	<0.001	54.0	(30.0–74.0)	54.0	(45.0–70.2)	<0.001
	N	**(%)**	***N***	**(%)**	***p*-value**	***N***	**(%)**	***N***	**(%)**	***p*-value**
Gender[2]										
Male/female	55/49	(53/47)	26/41	(39/61)	0.085	38/36	(51/49)	27/38	(42/58)	0.31
Surgery[2]										
No/yes/missing	22/81/1	(21/78/1)	12/55/0	(18/82/0)	0.70	14/60/0	(19/81/0)	12/53/0	(18/82/0)	1.00
Chemotherapy[2]										
No/yes/missing	76/27/1	(73/26/1)	48/19/0	(72/28/0)	0.86	57/17/0	(77/23/0)	49/16/0	(75/25/0)	0.84
Re-irradiation[2]										
No/yes/missing	95/7/2	(91/7/2)	64/3/0	(96/4/0)	0.74	69/4/1	(93/5/1)	64/1/0	(98/2/0)	0.37
Tumour location[3]										
Brain/skull base/other	50/53/1	(48/51/2)	32/34/1	(48/51/1)	0.46	37/37/0	(20/50/0)	29/35/1	(39/47/1)	0.49
Tumour histology[3]					0.68					0.63
High-grade glioma	25	(24)	13	(19)		16	(22)	11	(17)	
Low-grade glioma	16	(15)	11	(16)		11	(15)	11	(17)	
Meningioma	29	(28)	24	(36)		23	(31)	26	(40)	
Other	34	(33)	19	(28)		24	(32)	17	(26)	
Tumour location[3]					0.003					0.002
Temporal lobe	33	(32)	20	(30)		24	(32)	21	(32)	
Frontal lobe	25	(24)	15	(22)		20	(27)	15	(23)	
Parietal lobe	2	(2)	7	(10)		1	(1)	6	(9)	
Occipital lobe	3	(3)	1	(1)		3	(4)	0	0)	
Multiple lobes	23	(22)	3	(4)		16	(22)	3	(5)	
Other	18	(24)	21	(31)		10	(14)	20	(31)	
Tumour location[3]					0.42					0.57
Left hemisphere	32	(31)	24	(36)		21	(28)	24	(37)	
Right hemisphere	44	(42)	20	(30)		31	(42)	20	(31)	
Central	25	(24)	20	(30)		19	(26)	18	(28)	
Bilateral	3	(3)	3	(4)		3	(4)	3	(5)	

Abbreviations: N, number of patients; CTV, clinical target volume; RBE, relative biological effectiveness [1]Mann–Whitney *U* test, [2]Fisher's exact test, [3]χ^2 test.

Endpoint definition and extraction of dose-volume parameters

Those treatment-related side-effects that had been scored prospectively at all three PBT centres using the Common Terminology Criteria for Adverse Events (CTCAE) v.4 scoring system were considered (alopecia, dry eye syndrome, fatigue, headache, hearing and memory impairment, optic neuropathy). All patients were assessed at baseline and regular follow-up visits after PBT (3–12 months depending on the institution). To ensure a comparative evaluation between the centres, models for side-effects occurring at 12 months and 24 months after PBT were developed (Fig. 1). At 12 months following PBT, 104 and 67 patients were included in the exploration and validation cohort, respectively. At 24 months following PBT, 74 and 65 patients were included in the exploration and validation cohort, respectively. Drop-out at 24 months was caused by unavailable follow-up (exploration: n = 40; validation: n = 13), recurrent disease (exploration: n = 14; validation: n = 5) or death (exploration: n = 5 patients). Except for age in the exploration cohort, there were no significant differences in the patient characteristics between the scored patients and the drop-out at 12 or 24 months after PBT (Tables S2 and S3). Follow-up later than 24 months was not available for most patients.

For patients with a non-zero baseline toxicity value and an increase in severity after treatment, the follow-up severity score was used regardless of the pre-treatment value. If no increase in severity was observed, score zero was used. All endpoints were dichotomised at grade $\geq$ 1 (grade 0 vs remaining) and grade $\geq$ 2 (grade 0 and 1 vs remaining) at all time points. This choice was based on the distribution of observed severity grades, with low incidence of grade 2 for some and grade 3 for all considered side-effects.

The following OARs were associated with the evaluated endpoints: brain excluding target volume (brain-CTV), brainstem, cerebellum, chiasm, ipsilateral cochlea, hippocampi, ipsilateral lacrimal gland, optic nerves, skin (wall thickness 3 mm). In case they had not been delineated for treatment planning in advance, they were retrospectively contoured according to delineation guidelines by three radiation oncologists [34–38].

All dose distributions were retrospectively exported using RayStation® (RaySearch AB, Stockholm, Sweden) scripts. Absolute and relative volume parameters *VxGy(RBE)* [OAR volume in cm^3 or % receiving$x$ Gy(RBE)] and dose parameters *Dx%* [dose in x % of the OAR volume in Gy(RBE)] were extracted. For small OARs (volume < 10 cm^3), the near-maximum dose parameter *D2%* as well as median (*D50%*) and mean dose (D_{mean}) were analysed. All investigated side-effects, associated OARs and considered dosimetric parameters are given in Table S4.

Statistical analyses

Logistic regression was applied to assess the impact of dose-volume parameters and clinical variables on the toxicity endpoints. The clinical parameters comprised age at PBT, gender, prescribed total dose, target volume (CTV in cm^3), tumour location (brain or skull base), concurrent chemotherapy, and whether surgery was performed or not. Differences in binary, categorical, and continuous variables between the exploration and validation cohort were compared using exact Fisher tests, chi-squared tests, and Mann–Whitney-*U* tests, respectively. Correlations between dose-volume parameters were assessed using the Spearman correlation coefficient ρ. Two-sided tests were performed and SPSS Statistics 25 (IBM Corporation, Armonk, NY) was used. *P*-values <0.05 were considered statistically significant.

For the development and validation of NTCP models, the following steps were performed: (i) A 3-fold internal cross-validation was conducted 333 times on the exploration cohort to identify prognostic dose-volume parameters. (ii) Dose-volume parameters showing a significant association ($p < 0.05$) to the investigated endpoint in univariable logistic regression and the largest AUC value of the internal validation folds were pre-selected. (iii) Clinical parameters showing a significant association with the endpoint in logistic regression were tested for correlation with the dose-volume parameters selected during step (ii) using the Spearman correlation coefficient ρ. Multivariable logistic regression models containing the independent clinical parameters ($|\rho|$<0.5) and one dose-volume parameter were built as described in step (i). Uni- or multivariable models with the largest AUC value in internal cross-validation were selected as final NTCP models. (iv) The models derived from the exploration cohort were applied without changes to the validation cohort, i.e. the models were evaluated using the dose-volume parameters of the validation cohorts and the model coefficients derived from the exploration cohort. The 2.5th and 97.5th percentiles of 1000 bootstrap samples were used to

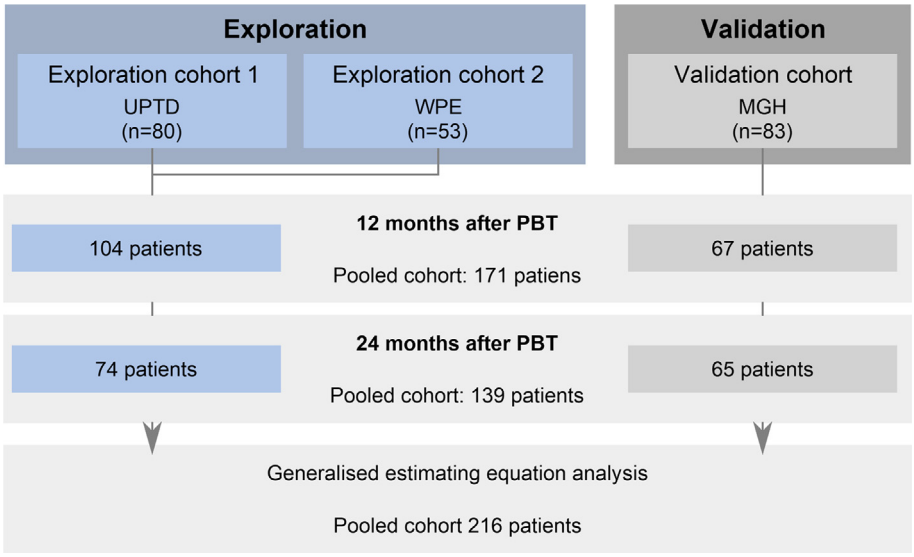

Fig. 1. Study design. UPTD, University Proton Therapy Dresden; MGH, Massachusetts General Hospital; PBT, proton beam therapy; WPE, West German Proton Therapy Centre Essen.

estimate the 95% confidence intervals (CI) of the AUC values. The prognostic performance was further assessed by calibration plots. In-house coded Python (version 2.7.10) programmes using the module scipy (statsmodels) were applied.

Since the incidence rates of various side-effects were low, additional exploratory analysis on the pooled data of all cohorts was conducted without external validation. Side-effects with at least 10 incidences were considered (Table S5). First, the dosimetric parameter of the model with the highest AUC value in univariable logistic regression was determined. Subsequently, this dosimetric parameter and all clinical cofactors that were significantly associated with the endpoint were included in multivariable models using stepwise forward variable selection based on likelihood ratio using a p-value of 0.05 for inclusion and 0.10 for exclusion (SPSS Statistics 25). The 95% confidence intervals of the AUC values are asymptotic estimates.

To consider patient data from all follow-up visits between 6 and 24 months following PBT, generalised estimating equations (GEEs) on the pooled cohort including 216 patients were set up (Tables S6). GEEs allow for the analysis of longitudinal data and account for the non-linear nature of the binary response as well as missing observations. A logit link function and an independent working correlation matrix were used. For each endpoint and dosimetric or clinical parameter, two GEEs were created. One included the dosimetric/clinical parameter and time as model predictors. The other included additionally the interaction between time and dosimetric/clinical parameter. Time was defined as natural numbers in the interval [1,7] representing the follow-up visits, for equidistant (three months) intervals starting with 1 at 6 months after PBT and ending with 7 at 24 months after PBT. For each side-effect and grade, the model revealing the lowest quasi log-likelihood estimate was selected (SPSS Statistics 25).

Results

Clinical characteristics of the development and validation cohort are presented in Table 1. The exploration cohort included patients with significantly larger CTVs, higher prescribed doses, and tumours involving more than one brain lobe.

Overall, the incidence rates of late side-effects at 12 and 24 months following PBT among patients with available follow-up were low (Table S7).

At 12 months after PBT, fatigue was the most common side-effect, with 36% and 26% of patients in the exploration and validation cohort reporting grade $\geq$ 1 fatigue, and 15% and 13% reporting grade $\geq$ 2, respectively. In three patients of the exploration cohort, optic neuropathy grade 4 was observed. The incidence rates of the side-effects were similar in both cohorts, except for dry eye syndrome (p = 0.034), which was observed in 10% of the exploration cohort but not in the validation cohort.

At 24 months following PBT, fatigue was still the most frequent side-effect. Hearing impairment and optic neuropathy grade 4 were observed in one and two patients of the exploration cohort, respectively. Fatigue (p = 0.004) and memory impairment (p = 0.011) occurred more often and with higher severity grade in the exploration cohort.

First, we developed and validated NTCP models using the independent development and validation cohorts (Table 2). For alopecia grade $\geq$ 1 at 12 months after PBT, the highest AUC value in cross-validation (AUC = 0.93, p < 0.001) was observed for two models, one including *V45Gy(RBE)* and the other *D2%* to the skin. Both parameters were highly correlated (ρ = 0.95). Alopecia was also associated with target volume, prescribed total dose, surgery, and target location in the skull base or brain (p < 0.02). However, including these parameters, the AUC did not increase further and the univariable model was selected (Fig. 2A). In external validation, the model including *D2%* performed slightly better (AUC = 0.77 [0.64–0.89]) and showed better calibration than the model including *V45Gy(RBE)* (AUC = 0.65 [0.47–0.83]). At 24 months after PBT, the models including *V30Gy(RBE)* (AUC = 0.80, p = 0.005) and *D2%* (AUC = 0.78, p < 0.001) to the skin showed the highest AUC value in cross-validation. These dosimetric parameters were highly correlated (ρ = 0.81). Both univariable models revealed high AUC values in external validation (*V30Gy(RBE)*: AUC = 0.90 [0.71–1.00] and *D2%*: AUC = 0.88 [0.69–1.00], respectively). However, external validation was challenging due to the low number of incidences in the validation cohort (Table S5). Hearing impairment grade $\geq$ 1 was significantly associated with age (exploration: p = 0.002, AUC = 0.83; validation: AUC = 0.73 [0.40–0.96]) at 12 months after PBT and with D_{mean} of the ipsilateral cochlea (exploration: p = 0.035, AUC = 0.75; validation: AUC = 0.87 [0.62–1.00]) at 24 months after PBT (Fig. 2B).

We then developed NTCP models based on the pooled cohorts (Table 3). For alopecia, significant associations with dosimetric

Table 2
NTCP models for late side-effects at 12 months and at 24 months following PBT. β_i are the regression coefficients of the logistic model.

Model	β_i	(95% CI)	p-value		AUC	(95% CI)
12 months after PBT						
Alopecia grade $\geq$ 1						
Skin *V45Gy(RBE)* in cm^{-3}	0.15	(0.08 to 0.22)	<0.001	Exploration	0.93	(0.85 to 1.00)
Constant	−1.80	(−2.63 to −1.13)		Validation	0.65	(0.47 to 0.83)
Skin *D2%* in $Gy(RBE)^{-1}$	0.15	(0.09 to 0.21)	<0.001	Exploration	0.93	(0.84 to 0.99)
Constant	−6.38	(−9.15 to −3.60)		Validation	0.77	(0.64 to 0.89)
24 months after PBT						
Alopecia grade $\geq$ 1						
Skin *V30Gy(RBE)* in cm^{-3}	0.048	(0.02 to 0.08)	0.003	Exploration	0.80	(0.62 to 0.95)
Constant	−1.70	(−2.52 to −0.88)		Validation	0.90	(0.71 to 1.00)
Skin *D2%* in $Gy(RBE)^{-1}$	0.068	(0.03 to 0.11)	0.001	Exploration	0.77	(0.60 to 0.93)
Constant	−3.18	(−4.74 to −1.62)		Validation	0.88	(0.69 to 1.00)
Hearing impairment grade $\geq$ 1						
Cochlea ipsilateral D_{mean} in $Gy(RBE)^{-1}$	0.038	(0.00 to 0.07)	0.035	Exploration	0.74	(0.42 to 1.00)
Constant	−3.03	(−4.47 to −1.58)		Validation	0.87	(0.62 to 1.00)

Abbreviations: AUC, area under the receiver operating characteristic curve; CI, confidence interval; D_{mean}, mean dose; *D2%*, dose in 2% of the volume; RBE, relative biological effectiveness; *VxGy(RBE)*, volume receiving *x* Gy(RBE).
Modelling of late side-effects following cranial proton beam therapy.

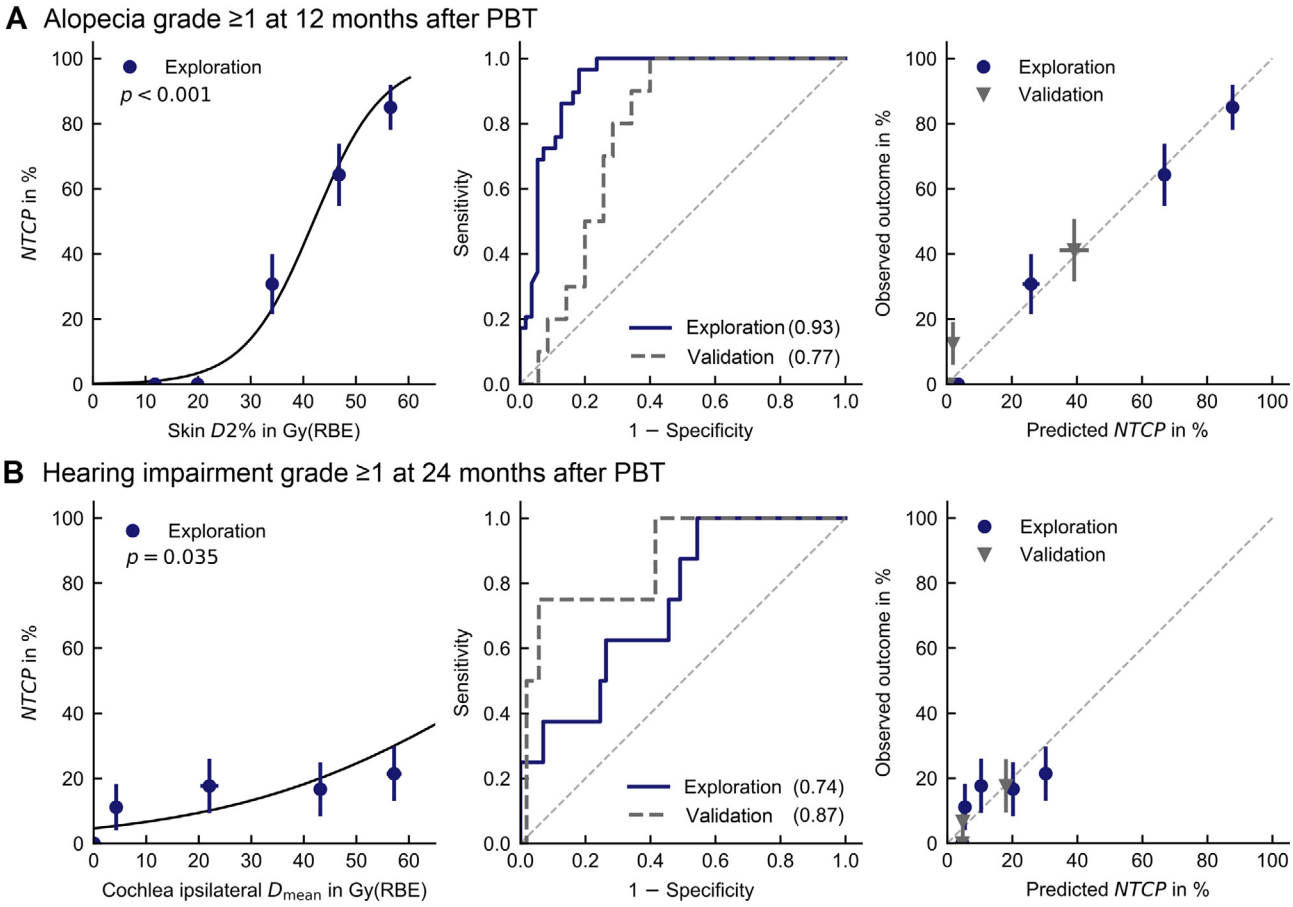

Fig. 2. NTCP models for (A) alopecia grade ≥ 1 at 12 months following PBT with the model parameters *D2%* to the skin and (B) hearing impairment grade ≥ 1 at 24 months following PBT depending on D_{mean} of the ipsilateral cochlea. Regression curves (left), ROC curves with AUC value in brackets (centre) and calibration plots (right) are displayed. Patients were sorted according to the parameter value and grouped into equally sized groups. Each data point and error bar represents the mean value and standard deviation of each patient group. NTCP, normal tissue complication probability.

parameters were observed, similar to the exploration/validation study. For hearing impairment grade ≥ 1, the associations with D_{mean} and age were also confirmed (Fig. 3A and B). In addition, for fatigue grade ≥ 1 at 24 months after PBT, a bivariable model including chemotherapy and *D2%* of the brainstem revealed the highest AUC value (0.68 [0.58–0.77], Fig. 3C). Patients receiving chemotherapy experienced less fatigue. Memory impairment grade ≥ 1 at 12 months after PBT was significantly associated with D_{mean} and *D2%* to the bilateral hippocampi ($p < 0.033$), *V20Gy(RBE)* of brain-CTV ($p = 0.040$) as well as *D2%* and *V20Gy(RBE)* to the cerebellum ($p < 0.043$). The model with the highest AUC value included the dosimetric parameter *D2%* to the hippocampi (AUC = 0.66 [0.55–0.77], Fig. 3D). For memory impairment grade ≥ 2 at 12 months, *V25Gy(RBE)* of brain-CTV was selected (AUC = 0.70 [0.52–0.88], Fig. 3E). At 24 months after PBT, memory impairment grade ≥ 1 was significantly related to dosimetric parameters to the brain-CTV (*V10Gy(RBE)* to *V50Gy(RBE)* and D_{mean}, $p < 0.035$). The model including *V35Gy(RBE)* revealed the highest AUC value (0.64 [0.52–0.75], $p = 0.014$, Fig. 3F).

No relations between dosimetric parameters and headache, optic neuropathy, and dry eye syndrome were observed.

Finally, we applied GEEs to the pooled cohorts, including the values at all available follow-up time points (Tables S8 and S9). The previously described dose–response relationships were confirmed. Furthermore, we observed the following associations: Dry eye syndrome grade ≥ 1 and grade ≥ 2 were significantly related to D_{mean} of the ipsilateral lacrimal gland. For dry eye syndrome grade ≥ 2, an additional association with the tumour location in brain or skull base was observed. Fatigue grade ≥ 1 was connected to *D2%* of the brainstem ($p = 0.028$) and *D2%* of the cerebellum ($p = 0.034$), but not to clinical cofactors. Headache grade ≥ 1 was related to age at treatment ($p = 0.010$), with younger age being associated with milder headaches. Memory impairment grade ≥ 1 was connected to several dosimetric parameters of different brain structures: brain-CTV [*D2%*, D_{mean}, *V10Gy(RBE)* to *V50Gy(RBE)*, $p < 0.004$], bilateral hippocampi (*D2%*, D_{mean}, $p < 0.016$), and cerebellum [*D2%*, D_{mean}, *V20Gy(RBE)* to *V40Gy(RBE)*, $p < 0.05$] as well as prescribed dose ($p = 0.012$) and CTV ($p = 0.042$). Memory impairment grade ≥ 2 was connected to D_{mean} of the bilateral hippocampi ($p = 0.032$) as well as certain dosimetric parameters of the brain-CTV [*D2%*, D_{mean}, *V10Gy(RBE)* to *V50Gy(RBE)*, $p < 0.014$]. Most side effects showed no temporal dependency.

Discussion

This study on adult patients treated with cranial PBT investigated the relation between late side-effects within two years following PBT and dose to associated OARs. Overall, PBT was well tolerated with very low incidence of grade ≥ 3 side-effects (<5%). Due to these low incidence rates, NTCP models were mainly developed for mild adverse effects which also have a significant impact to patient quality of life and are far more prevalent. Associations between mild alopecia and doses to the skin at both 12 and 24 months after PBT as well as mild hearing impairment and the

Table 3
NTCP models for late side-effects in the pooled analysis. The 95% confidence intervals of the AUC values are asymptotic estimates.

Model	β_i	(95% CI)	*p*-value	AUC	(95% CI)
12 months after PBT					
Alopecia grade $\geq$ 1					
Skin *D2%* in Gy(RBE)$^{-1}$	0.12	(0.08 to 0.15)	<0.001	0.90	(0.85 to 0.95)
Constant	−4.79	(−6.35 to −3.24)			
Memory impairment grade $\geq$ 1					
Hippocampi *D2%* in Gy(RBE)$^{-1}$	0.023	(0.004 to 0.043)	0.017	0.66	(0.55 to 0.77)
Constant	−2.32	(−3.12 to −1.51)			
Memory impairment grade $\geq$ 2					
Brain-CTV *V25Gy(RBE)**	5.02	(0.03 to 10.01)	0.049	0.70	(0.52 to 0.88)
Constant	−3.42	(−4.47 to −2.38)			
Hearing impairment grade $\geq$ 1					
Cochlea ipsi D_{mean} in Gy(RBE)$^{-1}$	0.032	(0.00 to 0.06)	0.021	0.82	(0.70 to 0.93)
Age in years	0.072	(0.03 to 0.12)	0.001		
Constant	−7.02	(−9.86 to −4.18)			
24 months after PBT					
Alopecia grade $\geq$ 1					
Skin *D2%* in Gy(RBE)$^{-1}$	0.078	(0.04 to 0.11)	<0.001	0.82	(0.75 to 0.89)
Constant	−3.80	(−5.26 to −2.34)			
Memory impairment grade $\geq$ 1					
Brain-CTV *V35Gy(RBE)**	6.50	(1.30 to 11.70)	0.014	0.64	(0.52 to 0.75)
Constant	−1.77	(−2.40 to −1.15)			
Fatigue grade $\geq$ 1					
Brainstem *D2%* in Gy(RBE)$^{-1}$	0.021	(0.00 to 0.04)	0.035	0.68	(0.58 to 0.77)
Chemotherapy	−1.16	(−2.30 to −0.02)	0.047		
Constant	−1.52	(−2.39 to −0.64)			
Hearing impairment grade $\geq$ 1					
Cochlea ipsi D_{mean} in Gy(RBE)$^{-1}$	0.050	(0.019 to 0.081)	0.001	0.79	(0.68 to 0.90)
Constant	−3.48	(−4.69 to −2.28)			

Abbreviations: AUC, area under the receiver operating characteristic curve; CI, confidence interval; CTV, clinical target volume; D_{mean}, mean dose; *D2%*, dose in 2% of the volume; RBE, relative biological effectiveness; *VxGy(RBE)*, volume receiving *x* Gy(RBE). *as fraction of the total volume.

mean dose to the ipsilateral cochlea at 24 months after PBT could be validated. In addition, the pooled analysis revealed dose–response relations between physician-rated memory impairment and intermediate to high doses to the remaining brain tissue as well as high doses to the hippocampi. Mild fatigue at 24 months after PBT was associated with high doses to the brainstem as well as chemotherapy, with patients who received chemotherapy reporting less fatigue. Furthermore, in time-dependent GEE analysis, dry eye syndrome was related to the mean dose of the ipsilateral lacrimal gland.

In general, the incidence rates of late effects in this study did not differ markedly from those reported in other studies [24,27,39,40]. Shih et al. [24] investigated late side-effects in 20 low-grade glioma patients treated with 54 Gy(RBE) passive scattering PBT. During follow-up (median: 5.1 years), the most common late side-effects were persistent headaches, fatigue, alopecia, and new neurologic deficits. Although mild headache (60%) and grade 3 fatigue (15%) were more common than in our study (10–15% and 2%, respectively), further results were similar.

The dose–response relationships for several late side-effects following PBT in this study were generally comparable with those of other dose–response studies on XRT data [41–44]. Alopecia after active scanning PBT was investigated by Palma et al. [23] in 116 adult brain tumour patients treated with a median dose of 54 Gy (RBE). They found *D2%* of the scalp as the only predictor for permanent alopecia. As this parameter was also found for alopecia grade $\geq$ 1 in the present study including both PBT techniques, it seems to be predictive for both active scanning and passive scattering PBT.

Mild hearing impairment was associated with the mean dose of the ipsilateral cochlea and age. Other studies reported similar causative factors in patients treated with XRT [42–46]. Asymmetric hearing loss more than 2 years after XRT was related to mean cochlear doses of more than 45 Gy [43] or 50 Gy [47] in patients without additional ototoxic treatment. De Marzi et al. [16] investigated 114 adult patients with chordoma and chondrosarcoma of the skull base treated with postoperative XRT and PBT (median dose 70 Gy(RBE), follow-up $\geq$ 26 months). Their logistic model predicting hearing impairment revealed an effective cochlear mean dose of ED_{50} = 56.0 Gy(RBE), compared to 79.4 Gy(RBE) and 69.8 Gy(RBE) for the models developed on the exploration cohort (Table 2) and the pooled cohorts (Table 3) in our study, respectively. These differences may be explained by the lower incidence rate and shorter follow-up in our study or by different toxicity assessment (physician-rated vs audiograms).

In the pooled cohort, memory impairment was related to intermediate and high doses to the remaining brain and to high doses to the hippocampi. Fairly low AUC values were observed; thus, these models need to be validated independently. Gondi et al. [13] investigated patients with benign or low-grade brain tumours and found a significant relationship between delayed recall at 18 months after XRT and the dosimetric parameter *D40%* of the bilateral hippocampi with ED_{50} = 14.88 Gy. Due to the rather unspecific nature of physician-rated memory impairment, it is challenging to establish dose–response relationships. Thus, more extensive objective tests are required to assess the neurocognitive function after PBT, such as the Wechsler Memory Scale or the Montreal Cognitive Assessment (MoCA) test [48–50].

Mild fatigue at 24 months after PBT was associated with the near-maximum dose to the brainstem and chemotherapy when analysing the pooled cohorts, requiring independent validation. In the PARSPORT Phase III trial, patients with acute fatigue grade $\geq$ 2 received higher doses to the brainstem, posterior fossa, and cerebellum compared to patients presenting grade $\leq$ 1 [51]. These patients were treated with intensity-modulated radiotherapy such that the brainstem dose was also associated with a low-dose bath in the posterior fossa. The effect of this dose bath on fatigue requires further investigations. However, no long-term data were acquired in this trial, as fatigue was not expected to be a late side-effect of RT [52]. Nevertheless, fatigue was a common

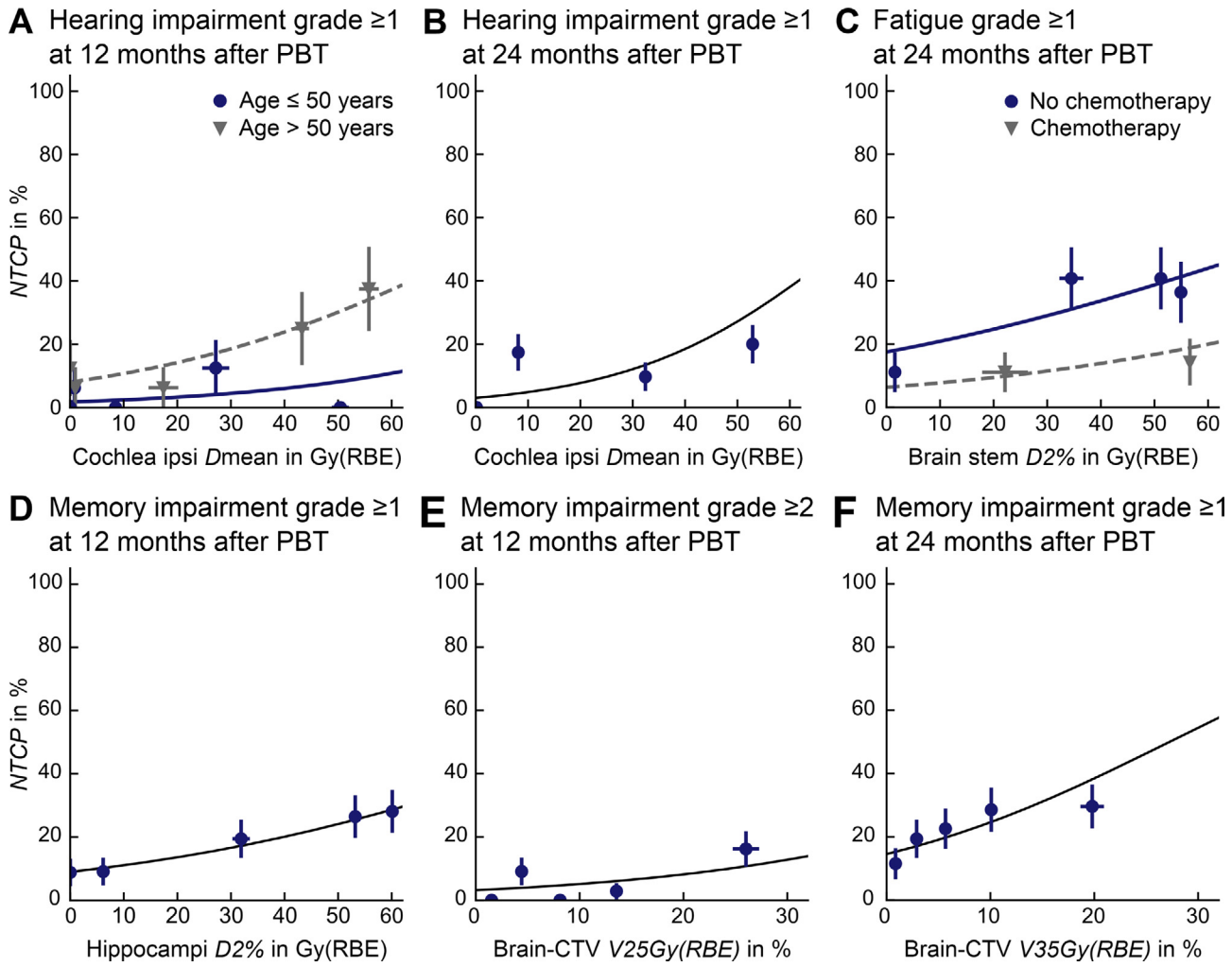

Fig. 3. NTCP models of the pooled analysis for (A) hearing impairment grade ≥ 1 at 12 months (B) hearing impairment grade ≥ 1 at 24 months, (C) fatigue grade ≥ 1 at 24 months following PBT, (D) memory impairment grade ≥ 1 at 12 months following PBT, (E) memory impairment grade ≥ 2 at 12 months following PBT, and (F) memory impairment grade ≥ 1 at 24 months following PBT. Patients were sorted according to the parameter value and grouped into equally sized groups. Each data point and error bar represents the mean value and standard deviation of each patient group. For models (A, C) two regression curves are shown for groups of different age and chemotherapy application, respectively. NTCP, normal tissue complication probability.

late side-effect in our study as described before [53]. The lack of studies on dose–response relationships regarding chronic fatigue may be explained by the assumption that this side-effect could be caused synergistically by many influencing factors including biochemical factors, psychological disturbances such as depression or anxiety, further therapies such as chemotherapy, hormone therapy or surgery, or comorbidities such as pain or electrolytic disturbances [53]. In this study, patients treated with chemotherapy were found to present with lower fatigue than others, which was also observed in a study on lung cancer patients [54]. However, other studies showed no association of chemotherapy with fatigue [55], and others even showed an opposite association [56]. Because of these controversies, the relationships between fatigue and potential predictive factors should be investigated in larger cohorts including QoL questionnaires.

Dry eye syndrome was associated with the mean dose of the ipsilateral lacrimal gland in GEE analysis of the pooled cohort, requiring independent validation. Although this result is in accordance with other studies [20,57], a comprehensive assessment including specific questionnaires and/or objective testing of the tear film could be included in future studies as dry eye syndrome affects patients' quality of life [58].

NTCP modelling was limited mainly due to the low incidence rates of several side-effects, the low doses received by some of the OARs and the still rather short follow-up time compared to the onset of some investigated side-effects.

Still, NTCP models and dose limits are required for treatment planning to further reduce the observed side-effects. An increasing number of patients is treated within ongoing clinical trials (e.g. NCT02824731 [59]), whose data can be used to validate the presented NTCP models. To accelerate translational research, large multicentre studies are required. Rapid acquisition of high-quality data including patient data, outcome data, irradiation data and medical imaging could be achieved, for example, using federated databases [60,61]. Furthermore, the cohorts were rather heterogeneous concerning tumour histology. However, two years after therapy, many patients were still alive, even with high-grade tumours.

All dosimetric parameters were based on the planned dose distribution. Obviously, slight positioning errors could result in deviations in the delivered dose from the planned dose, especially in small OARs. However, since positioning is mainly based on planar X-ray imaging, the three-dimensional analysis of setup errors is impossible. Moreover, inter-observer variations in the delineation

of OARs may alter dosimetric parameters, although standardised delineation guidelines were used in this study [62–64]. Furthermore, toxicity assessment is subject to interobserver variability, even if the same scoring system is used. Some side-effects requiring extensive examination were not investigated, e.g. endocrine dysfunction [16,24] or several cranial neuropathies [65,66]. Moreover, fatigue and memory impairment could also be impacted by other patient- and treatment-related factors, such as psychosocial effects of the malignant diagnosis, epilepsy or antiepileptic drugs, which were not available in this study. Biological differences between XRT and PBT may occur due to a variable linear energy transfer and RBE for proton beams [67–69]. These parameters should be considered in future PBT-based NTCP models.

In conclusion, we developed NTCP models for late side-effects following cranial PBT. In part, these NTCP models were validated externally. In the validation study, alopecia was associated with dose-volume parameters of the skin, while hearing impairment was related to cochlear doses. Using the pooled cohort, dose–response relations between late physician-rated memory impairment and the dose to the remaining brain as well as the hippocampi were observed. Late fatigue was related to brainstem dose and chemotherapy, and dry eye syndrome was associated with the mean dose of the ipsilateral lacrimal gland. After validation of these NTCP models using large updated long-term databases, they may be part of a reliable tool for future treatment selection for PBT.

Disclaimers

None.

Acknowledgements

The excellent work of the clinical trials offices under the direction of Monique Falk and Daniel Büttner in Dresden and Stefanie Schulze-Schleithoff in Essen as well as the clinical staff is highly acknowledged, including the work of Sabine Frisch for data collection and transfer. We thank all patients who volunteered to participate in the studies. The work was partially supported by the Else Kröner-Fresenius Foundation (RB).

Conflicts of interest

In the past 5 years, Dr. Michael Baumann attended an advisory board meeting of MERCK KGaA (Darmstadt), for which the University of Dresden received a travel grant. He further received funding for his research projects and for educational grants to the University of Dresden by Teutopharma GmbH (2011-2015), IBA (2016), Bayer AG (2016-2018), Merck KGaA (2014-open), Medipan GmbH (2014-2018). He is on the supervisory board of HI-STEM gGmbH (Heidelberg) for the German Cancer Research Center (DKFZ, Heidelberg) and also member of the supervisory body of the Charité University Hospital, Berlin. As former chair of OncoRay (Dresden) and present CEO and Scientific Chair of the German Cancer Research Center (DKFZ, Heidelberg), he has been or is still responsible for collaborations with a multitude of companies and institutions, worldwide. In this capacity, he discussed potential projects with and has signed/signs contracts for his institute(s) and for the staff for research funding and/or collaborations with industry and academia, worldwide, including but not limited to pharmaceutical corporations like Bayer, Boehringer Ingelheim, Bosch, Roche and other corporations like Siemens, IBA, Varian, Elekta, Bruker and others. In this role, he was/is further responsible for commercial technology transfer activities of his institute(s), including the DKFZ-PSMA617 related patent portfolio [WO2015055318 (A1), ANTIGEN (PSMA)] and similar IP portfolios. Dr. Baumann confirms that, to the best of his knowledge, none of the above funding sources was involved in the preparation of this paper.

In the past 5 years, Dr. Krause received funding for her research projects by IBA (2016), Merck KGaA (2014-2018 for preclinical study; 2018-2020 for clinical study), Medipan GmbH (2014-2018) and by the Gert and Susanna Mayer Foundation (2019-2022). In the past 5 years, Dr. Troost, Dr. Krause and Dr. Löck have been involved in an ongoing publicly funded (German Federal Ministry of Education and Research) project with the companies Medipan, Attomol GmbH, GA Generic Assays GmbH, Gesellschaft für medizinische und wissenschaftliche genetische Analysen, Lipotype GmbH and PolyAn GmbH (2019-2021). For the present manuscript, none of the above mentioned funding sources were involved.

Appendix A. Supplementary data

Supplementary data to this article can be found online at https://doi.org/10.1016/j.radonc.2021.01.004.

References

[1] Baumann M, Krause M, Overgaard J, et al. Radiation oncology in the era of precision medicine. Nat Rev Cancer 2016;16:234.
[2] Harrabi SB, Bougatf N, Mohr A, et al. Dosimetric advantages of proton therapy over conventional radiotherapy with photons in young patients and adults with low-grade glioma. Strahlenther Onkol 2016;192:759–69.
[3] Kristensen I, Nilsson K, Nilsson P. Comparative proton and photon treatment planning in pediatric patients with various diagnoses. Int J Part Ther 2015;2:367–75.
[4] Palm Å, Johansson KA. A review of the impact of photon and proton external beam radiotherapy treatment modalities on the dose distribution in field and out-of-field; Implications for the long-term morbidity of cancer survivors. Acta Oncol 2007;46:462–73.
[5] Verma V, Simone II CB, Mishra MV. Quality of life and patient-reported outcomes following proton radiation therapy: A systematic review. J Natl Cancer Inst 2018;110. djx208–djx208.
[6] Particle Therapy Co-Operative Group. Particle therapy facilities in operation. [cited 2020 May 07], 2020. URL: https://www.ptcog.ch/index.php/facilities-in-operation.
[7] Langendijk JA, Lambin P, De Ruysscher D, Widder J, Bos M, Verheij M. Selection of patients for radiotherapy with protons aiming at reduction of side effects: the model-based approach. Radiother Oncol 2013;107:267–73.
[8] Quik E, Feenstra T, Postmus D, et al. Individual patient information to select patients for different radiation techniques. Eur J Cancer 2016;62:18–27.
[9] Widder J, van der Schaaf A, Lambin P, et al. The quest for evidence for proton therapy: Model-based approach and precision medicine. Int J Radiat Oncol Biol Phys 2016;95:30–6.
[10] Burman C, Kutcher G, Emami B, Goitein M. Fitting of normal tissue tolerance data to an analytic function. Int J Radiat Oncol Biol Phys 1991;21:123–35.
[11] Bender ET. Brain necrosis after fractionated radiation therapy: Is the halftime for repair longer than we thought?. Med Phys 2012;39:7055–61.
[12] Lawrence YR, Li XA, el Naqa I, et al. Radiation dose-volume effects in the brain. Int J Radiat Oncol Biol Phys 2010;76:S20–7.
[13] Gondi V, Hermann BP, Mehta MP, Tomé WA. Hippocampal dosimetry predicts neurocognitive function impairment after fractionated stereotactic radiotherapy for benign or low-grade adult brain tumors. Int J Radiat Oncol Biol Phys 2012;83:e487–93.
[14] Meeks SL, Buatti JM, Foote KD, Friedman WA, Bova FJ. Calculation of cranial nerve complication probability for acoustic neuroma radiosurgery. Int J Radiat Oncol Biol Phys 2000;47:597–602.
[15] Pai HH, Thornton A, Katznelson L, et al. Hypothalamic/pituitary function following high-dose conformal radiotherapy to the base of skull: Demonstration of a dose-effect relationship using dose-volume histogram analysis. Int J Radiat Oncol Biol Phys 2001;49:1079–92.
[16] De Marzi L, Feuvret L, Boulé T, et al. Use of gEUD for predicting ear and pituitary gland damage following proton and photon radiation therapy. Br J Radiol 2015;88:20140413.
[17] Lee TF, Yeh SA, Chao PJ, et al. Normal tissue complication probability modeling for cochlea constraints to avoid causing tinnitus after head-and-neck intensity-modulated radiation therapy. Radiat Oncol 2015;10:194.
[18] Martel MK, Sandler HM, Cornblath WT, et al. Dose-volume complication analysis for visual pathway structures of patients with advanced paranasal sinus tumors. Int J Radiat Oncol Biol Phys 1997;38:273–84.
[19] Mayo C, Martel MK, Marks LB, Flickinger J, Nam J, Kirkpatrick J. Radiation dose-volume effects of optic nerves and chiasm. Int J Radiat Oncol Biol Phys 2010;76:S28–35.
[20] Batth SS, Sreeraman R, Dienes E, et al. Clinical-dosimetric relationship between lacrimal gland dose and ocular toxicity after intensity-modulated radiotherapy for sinonasal tumours. Br J Radiol 2013;86:20130459.

[21] Blanchard P, Wong AJ, Gunn GB, et al. Toward a model-based patient selection strategy for proton therapy: External validation of photon-derived normal tissue complication probability models in a head and neck proton therapy cohort. Radiother Oncol 2016;121:381–6.
[22] Pedersen J, Flampouri S, Bryant C, et al. Cross-modality applicability of rectal normal tissue complication probability models from photon- to proton-based radiotherapy. Radiother Oncol 2020;142:253–60.
[23] Palma G, Taffelli A, Fellin F, et al. Modelling the risk of radiation induced alopecia in brain tumor patients treated with scanned proton beams. Radiother Oncol 2020;144:127–34.
[24] Shih HA, Sherman JC, Nachtigall LB, et al. Proton therapy for low-grade gliomas: results from a prospective trial. Cancer 2015;121:1712–9.
[25] Grosshans DR, Zhu XR, Melancon A, et al. Spot scanning proton therapy for malignancies of the base of skull: Treatment planning, acute toxicities, and preliminary clinical outcomes. Int J Radiat Oncol Biol Phys 2014;90:540–6.
[26] Hauswald H, Rieken S, Ecker S, et al. First experiences in treatment of low-grade glioma grade I and II with proton therapy. Radiat Oncol 2012;7:189.
[27] Weber DC, Schneider R, Goitein G, et al. Spot scanning-based proton therapy for intracranial meningioma: long-term results from the Paul Scherrer Institute. Int J Radiat Oncol Biol Phys 2012;83:865–71.
[28] Combs SE, Kessel K, Habermehl D, Haberer T, Jäkel O, Debus J. Proton and carbon ion radiotherapy for primary brain tumors and tumors of the skull base. Acta Oncol 2013;52:1504–9.
[29] Williamson D, Gonzalez M, Finlay A. The effect of hair loss on quality of life. J Eur Acad Dermatol Venereol 2001;15:137–9.
[30] DRKS00007670. Proton therapy of brain tumors: Prospective collection of effectiveness and side effects with standard clinical doses (Proto-R-Hirn). German Clinical Trials Center [Internet], Cologne: German Institute of Medical Documentation and Information (Germany), 2008. Identifier DRKS00007670 [registered 2015 Feb 02, cited 2020 May 07], 2015. URL: https://www.drks.de/drks_web/navigate.do?navigationId=trial.HTML&TRIAL_ID=DRKS00007670.
[31] DRKS00008569. Proton therapy of skull base tumors: Prospective collection of effectiveness and side effects with standard clinical doses (Proto-R-Schädelbasis). German Clinical Trials Center [Internet], Cologne: German Institute of Medical Documentation and Information (Germany), 2008. Identifier DRKS00008569 [registered 2015 May 21, cited 2020 May 07], 2015. URL: https://www.drks.de/drks_web/navigate.do?navigationId=trial.HTML&TRIAL_ID=DRKS00008569.
[32] DRKS00004384. Register study standard proton therapy WPE- Adults - (ProReg). German Clinical Trials Center [Internet], Cologne: German Institute of Medical Documentation and Information (Germany), 2008. Identifier: DRKS00004384 [registered 2012 Sep 28, cited 2020 May 07] , 2012. URL: https://www.drks.de/drks_web/navigate.do?navigationId=trial.HTML&TRIAL_ID=DRKS00004384.
[33] Dutz A, Lühr A, Agolli L, et al. Development and validation of NTCP models for acute side-effects resulting from proton beam therapy of brain tumours. Radiother Oncol 2019;130:164–71.
[34] Schmahmann JD, Doyon J, McDonald D, et al. Three-dimensional MRI atlas of the human cerebellum in proportional stereotaxic space. Neuroimage 1999;10:233–60.
[35] Chera BS, Amdur RJ, Patel P, Mendenhall WM. A radiation oncologists guide to contouring the hippocampus. Am J Clin Oncol 2009;32:20–2.
[36] Sun Y, Yu XL, Luo W, et al. Recommendation for a contouring method and atlas of organs at risk in nasopharyngeal carcinoma patients receiving intensity-modulated radiotherapy. Radiother Oncol 2014;110:390–7.
[37] Scoccianti S, Detti B, Gadda D, et al. Organs at risk in the brain and their dose-constraints in adults and in children: A radiation oncologist's guide for delineation in everyday practice. Radiother Oncol 2015;114:230–8.
[38] Eekers DBP, in't Ven L, Roelofs E, et al. The EPTN consensus-based atlas for CT- and MR-based contouring in neuro-oncology. Radiother Oncol 2018;128:37–43.
[39] Noël G, Bollet MA, Calugaru V, et al. Functional outcome of patients with benign meningioma treated by 3D conformal irradiation with a combination of photons and protons. Int J Radiat Oncol Biol Phys 2005;62:1412–22.
[40] Weber DC, Badiyan S, Malyapa R, et al. Long-term outcomes and prognostic factors of skull-base chondrosarcoma patients treated with pencil-beam scanning proton therapy at the Paul Scherrer Institute. Neuro Oncol 2016;18:236–43.
[41] Lawenda BD, Gagne HM, Gierga DP, et al. Permanent alopecia after cranial irradiation: dose-response relationship. Int J Radiat Oncol Biol Phys 2004;60:879–87.
[42] Bhandare N, Jackson A, Eisbruch A, et al. Radiation therapy and hearing loss. Int J Radiat Oncol Biol Phys 2010;76:S50–7.
[43] Pan CC, Eisbruch A, Lee JS, Snorrason RM, Ten Haken RK, Kileny PR. Prospective study of inner ear radiation dose and hearing loss in head-and-neck cancer patients. Int J Radiat Oncol Biol Phys 2005;61:1393–402.
[44] Honoré HB, Bentzen SM, Møller K, Grau C. Sensori-neural hearing loss after radiotherapy for nasopharyngeal carcinoma: Individualized risk estimation. Radiother Oncol 2002;65:9–16.
[45] Ho WK, Wei WI, Kwong DL, et al. Long-term sensorineural hearing deficit following radiotherapy in patients suffering from nasopharyngeal carcinoma: a prospective study. Head Neck 1999;21:547–53.
[46] Bhandare N, Antonelli PJ, Morris CG, Malayapa RS, Mendenhall WM. Ototoxicity after radiotherapy for head and neck tumors. Int J Radiat Oncol Biol Phys 2007;67:469–79.
[47] van der Putten L, de Bree R, Plukker JT, et al. Permanent unilateral hearing loss after radiotherapy for parotid gland tumors. Head Neck 2006;28:902–8.
[48] Wechsler D. A standardized memory scale for clinical use. J Psychol 1945;19:87–95.
[49] Nasreddine ZS, Phillips NA, Bédirian V, et al. The Montreal cognitive assessment, MoCA: A brief screening tool for mild cognitive impairment. J Am Geriatr Soc 2005;53:695–9.
[50] Dutz A, Agolli L, Bütof R, et al. Neurocognitive function and quality of life after proton beam therapy for brain tumour patients. Radiother Oncol 2020;143:108–16.
[51] Gulliford SL, Miah AB, Brennan S, et al. Dosimetric explanations of fatigue in head and neck radiotherapy: an analysis from the PARSPORT Phase III trial. Radiother Oncol 2012;104:205–12.
[52] Nutting CM, Morden JP, Harrington KJ, et al. Parotid-sparing intensity modulated versus conventional radiotherapy in head and neck cancer (PARSPORT): A phase 3 multicentre randomised controlled trial. Lancet Oncol 2011;12:127–36.
[53] Jereczek-Fossa BA, Marsiglia HR, Orecchia R. Radiotherapy-related fatigue. Crit Rev Oncol Hematol 2002;41:317–25.
[54] Hickok JT, Morrow GR, McDonald S, Bellg AJ. Frequency and correlates of fatigue in lung cancer patients receiving radiation therapy: Implications for management. J Pain Symptom Manage 1996;11:370–7.
[55] Ferris MJ, Zhong J, Switchenko JM, et al. Brainstem dose is associated with patient-reported acute fatigue in head and neck cancer radiation therapy. Radiother Oncol 2018;126:100–6.
[56] Bower JE, Ganz PA, Irwin MR, Kwan L, Breen EC, Cole SW. Inflammation and behavioral symptoms after breast cancer treatment: do fatigue, depression, and sleep disturbance share a common underlying mechanism?. J Clin Oncol 2011;29:3517–22.
[57] Bhandare N, Moiseenko V, Song WY, Morris CG, Bhatti MT, Mendenhall WM. Severe dry eye syndrome after radiotherapy for head-and-neck tumors. Int J Radiat Oncol Biol Phys 2012;82:1501–8.
[58] Grubbs JRJ, Tolleson-Rinehart S, Huynh K, Davis RM. A review of quality of life measures in dry eye questionnaires. Cornea 2014;33:215–8.
[59] NCT02824731. Comparison of proton and photon radiotherapy of brain tumors (ProtoChoice-Hirn). ClinicalTrials.gov [Internet], Bethesda (MD): National Library of Medicine (US), 2000 Feb 29. Identifier NCT02824731 [registered 2016 July 07, updated 2019 Feb 18, cited 2020 May 07], 2016. URL: https://clinicaltrials.gov/ct2/show/NCT02824731.
[60] Skripcak T, Belka C, Bosch W, et al. Creating a data exchange strategy for radiotherapy research: Towards federated databases and anonymised public datasets. Radiother Oncol 2014;113:303–9.
[61] Lühr A, von Neubeck C, Pawelke J, et al. "Radiobiology of Proton Therapy": Results of an international expert workshop. Radiother Oncol 2018;128:56–67.
[62] Foppiano F, Fiorino C, Frezza G, Greco C, Valdagni R. The impact of contouring uncertainty on rectal 3D dose-volume data: Results of a dummy run in a multicenter trial (AIROPROS01-02). Int J Radiat Oncol Biol Phys 2003;57:573–9.
[63] Rosewall T, Bayley AJ, Chung P, et al. The effect of delineation method and observer variability on bladder dose-volume histograms for prostate intensity modulated radiotherapy. Radiother Oncol 2011;101:479–85.
[64] Nelms BE, Tomé WA, Robinson G, Wheeler J. Variations in the contouring of organs at risk: test case from a patient with oropharyngeal cancer. Int J Radiat Oncol Biol Phys 2012;82:368–78.
[65] Lin YS, Jen YM, Lin JC. Radiation-related cranial nerve palsy in patients with nasopharyngeal carcinoma. Cancer 2002;95:404–9.
[66] Kong L, Lu JJ, Liss AL, et al. Radiation-induced cranial nerve palsy: A cross-sectional study of nasopharyngeal cancer patients after definitive radiotherapy. Int J Radiat Oncol Biol Phys 2011;79:1421–7.
[67] Lühr A, von Neubeck C, Krause M, Troost EGC. Relative biological effectiveness in proton beam therapy – current knowledge and future challenges. Clin Transl Radiat Oncol 2018;9:35–41.
[68] Paganetti H. Relative biological effectiveness (RBE) values for proton beam therapy. Variations as a function of biological endpoint, dose, and linear energy transfer. Phys Med Biol 2014;59:R419–72.
[69] Eulitz J, Troost E, Raschke F, et al. Predicting late magnetic resonance image changes in glioma patients after proton therapy. Acta Oncol 2019;58:1536–9.